Article

Cell Reports

Adaptive Evolution of Gene Expression in *Drosophila*

Graphical Abstract

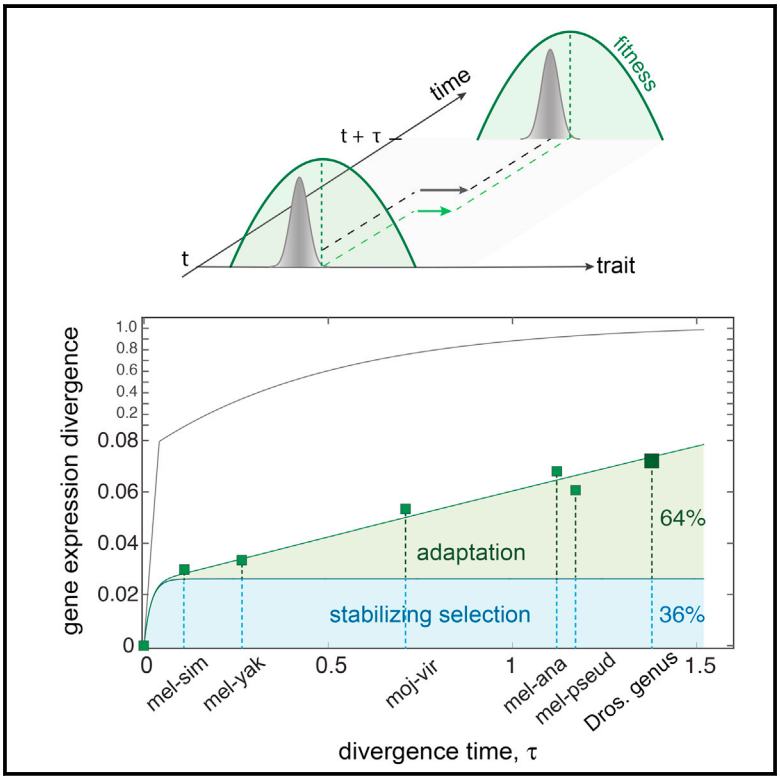

Authors

Armita Nourmohammad, Joachim Rambeau, Torsten Held, Viera Kovacova, Johannes Berg, Michael Lässig

Correspondence

armitan@princeton.edu (A.N.), mlassig@uni-koeln.de (M.L.)

In Brief

Drosophila presents an evolutionary conundrum: there is ubiquitous genomic adaptation, yet it has been impossible to identify system-wide signals of adaptation for gene expression. Nourmohammad et al. develop a method to infer stabilizing and directional selection from expression data. They show that adaptation dominates the evolution of gene expression in *Drosophila.*

Highlights

- Adaptive evolution of gene expression is pervasive in *Drosophila*
- Stabilization and adaptation of gene expression follow distinct molecular clocks
- Gene function determines the rate of expression adaptation
- Sex-specific adaptation of gene expression occurs predominantly in males

Nourmohammad et al., 2017, Cell Reports *20*, 1385–1395
August 8, 2017
http://dx.doi.org/10.1016/j.celrep.2017.07.033

Cell Reports
Article

Adaptive Evolution of Gene Expression in *Drosophila*

Armita Nourmohammad,[1,4,*] Joachim Rambeau,[2] Torsten Held,[2] Viera Kovacova,[3] Johannes Berg,[2] and Michael Lässig[2,*]
[1]Joseph-Henri Laboratories of Physics and Lewis-Sigler Institute for Integrative Genomics, Princeton University, Princeton, NJ 08544, USA
[2]Institut für Theoretische Physik, Universität zu Köln, Zülpicher Str. 77, 50937 Köln, Germany
[3]CECAD, Universität zu Köln, Joseph-Stelzmann-Str. 26, 50931 Köln, Germany
[4]Lead Contact
*Correspondence: armitan@princeton.edu (A.N.), mlassig@uni-koeln.de (M.L.)
http://dx.doi.org/10.1016/j.celrep.2017.07.033

SUMMARY

Gene expression levels are important quantitative traits that link genotypes to molecular functions and fitness. In *Drosophila*, population-genetic studies have revealed substantial adaptive evolution at the genomic level, but the evolutionary modes of gene expression remain controversial. Here, we present evidence that adaptation dominates the evolution of gene expression levels in flies. We show that 64% of the observed expression divergence across seven *Drosophila* species are adaptive changes driven by directional selection. Our results are derived from time-resolved data of gene expression divergence across a family of related species, using a probabilistic inference method for gene-specific selection. Adaptive gene expression is stronger in specific functional classes, including regulation, sensory perception, sexual behavior, and morphology. Moreover, we identify a large group of genes with sex-specific adaptation of expression, which predominantly occurs in males. Our analysis opens an avenue to map system-wide selection on molecular quantitative traits independently of their genetic basis.

INTRODUCTION

Several studies have found evidence for widespread adaptive evolution of the *Drosophila* genome (Andolfatto, 2005; Mustonen and Lässig, 2007; Sella et al., 2009). This includes adaptive changes in the non-coding sequence, consistent with classical ideas on the importance of regulatory evolution for phenotypic adaptation (King and Wilson, 1975). Gene expression levels are important molecular phenotypes that quantify the effects of regulation on organismic traits and fitness. Insights on how genome evolution affects gene expression have come from studies of quantitative trait loci (QTLs); see Fraser (2011); Romero et al. (2012), and Pai et al. (2015) for reviews. These studies compare lineage- or species-specific difference in the expression QTLs, in line with Orr's sign test for selection on quantitative traits (Orr, 1998). Due to the limited number of QTLs, the sign test is only applicable to gene groups that have been pre-determined based on criteria other than selection on expression levels. In yeast, at least 10% of the genes have been inferred to undergo adaptive evolution of expression (Fraser et al., 2010). By extending the sign test to include information on outgroup species, it has been possible to identify lineage-specific positive selection on *cis*-regulatory expression QTLs in functional gene classes of mice (Fraser et al., 2011) and plants (Riedel et al., 2015). A similar approach has been used to correlate population-specific environmental variables with expression SNPs; this has shown that local adaptation of the human population is driven by gene expression in a number of gene classes (Fraser, 2013). In flies, expression-QTL analysis has been used to estimate *cis* and *trans* effects on expression (Genissel et al., 2008; Wittkopp et al., 2008) and to compare the evolution of expression and that of the underlying regulatory sequence (Coolon et al., 2014); related studies have been performed in yeast (Bullard et al., 2010; Artieri and Fraser, 2014). These QTL studies have brought specific insights into modes of gene expression evolution in specific functional classes. However, given the complexity of the regulatory genotype-to-phenotype map and the limited sensitivity of QTL studies, our understanding of how genome-wide adaptive changes relate to mRNA and protein levels has remained incomplete (Hoekstra and Coyne, 2007; Fraser, 2011; Pai et al., 2015).

An alternative approach is to analyze the evolution of gene expression by methods of quantitative genetics, without explicit reference to genetic evolution of the QTL (Rifkin et al., 2003; Khaitovich et al., 2004, 2005; Lemos et al., 2005; Rifkin et al., 2005; Gilad et al., 2006; Whitehead and Crawford, 2006; Zhang et al., 2007; Bedford and Hartl, 2009; Fraser et al., 2011; Romero et al., 2012; Pai et al., 2015). These studies compare the expression divergence across species, the variation within species, and the expected behavior for neutral evolution (Lynch and Hill, 1986). A broad picture of evolutionary constraint on gene expression levels caused by stabilizing selection has emerged in a number of species, including *Drosophila* (Rifkin et al., 2003; Lemos et al., 2005; Rifkin et al., 2005; Gilad et al., 2006; Bedford and Hartl, 2009; Romero et al., 2012). Mutation accumulation experiments in *Drosophila* show that the neutral expression divergence generated by random mutations in the lab significantly exceeds the natural expression variation, indicating strong negative selection on most random mutations affecting gene expression (Rifkin et al., 2005). A comparative study between human and chimpanzee has produced signatures of predominantly neutral evolution of gene expression (Khaitovich et al., 2004, 2005). Other studies in primates have identified stabilizing selection, as well

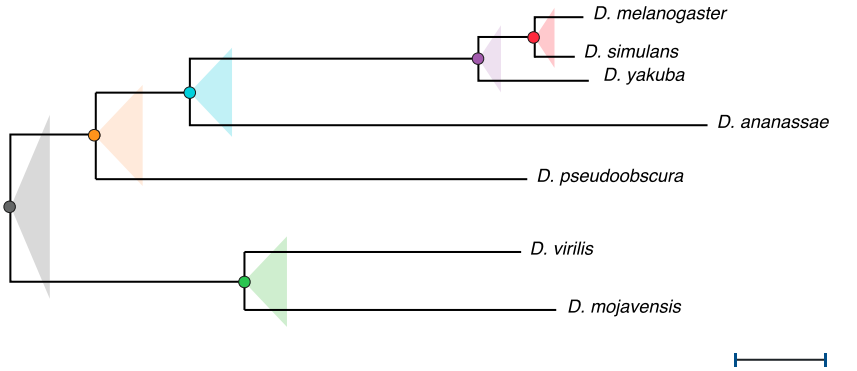

clade	mel - sim	mel - yak	moj- vir	mel - ana	mel - pse	mel - moj (Dros.)
time, τ_c	0.11	0.27	0.71	1.12	1.17	1.38
species	*D. melanogaster* *D. simulans*	*D. melanogaster* *D. simulans* *D.yakuba*	*D. mojavensis* *D. virilis*	*D. melanogaster* *D. simulans* *D.yakuba* *D. ananassae*	*D. melanogaster* *D. simulans* *D.yakuba* *D. ananassae* *D. pseudoobscura*	*D. melanogaster* *D. simulans* *D.yakuba* *D. ananassae* *D. pseudoobscura* *D. mojavensis* *D. virilis*

Figure 1. Phylogenetic Tree and Evolutionary Distances of 7 *Drosophila* Species

Phylogeny of the *Drosophila* genus, as reconstructed in Drosophila 12 Genomes Consortium et al. (2007) from synonymous sequence divergence. Six clades are marked by colored triangles; their ancestral nodes are marked by colored circles. The table specifies the species contained in each of the clades and the clade divergence time τ_C (see Experimental Procedures).

as lineage- and tissue-specific directional expression changes (Gilad et al., 2006; Blekhman et al., 2008; Brawand et al., 2011; Romero et al., 2012). However, it has remained difficult to demonstrate that positive selection, as opposed to relaxed stabilizing selection, is the evolutionary cause of expression divergence (Fraser, 2011). Thus, estimating the genome-wide contribution of adaptation to the evolution of gene expression is an outstanding problem.

In this paper, we show that adaptation is the prevalent evolutionary mode of gene expression in the *Drosophila* genus. We infer directional selection driving adaptation, together with conservation under stabilizing selection, and we show that these forces act on different scales of evolutionary time. Our inference is based on theoretical results on the evolution of molecular quantitative traits (Held et al., 2014; Nourmohammad et al., 2013a, 2013b), using solely the dependence of gene expression divergence on the divergence time of 7 *Drosophila* species. Moreover, the method only relies on the phenotypic observables and does not depend on number and effects of the underlying QTL; these molecular determinants of gene expression are often unknown and vary considerably among genes.

RESULTS

Pattern of Gene Expression Divergence

We use gene expression data from samples of males and females (Zhang et al., 2007), which cover 6,332 orthologous genes in seven *Drosophila* species. A phylogenetic tree of these species is shown in Figure 1. The dataset of Zhang et al. (2007) is obtained from species-specific microarrays, which makes it suited to cross-species analysis. Gene expression levels are defined by a standard transformation of mRNA counts, which accounts for differences in assay sensitivity among experimental probes (Quackenbush, 2002). The transformation method and its implications for evolutionary analysis are detailed in Experimental Procedures and Supplemental Experimental Procedures (Figure S1). We use these data to estimate the mean expression level of a gene within each species, its total heritable expression variance Δ (referred to as expression diversity), and its non-heritable expression variance between biological replicates. For each pair of species, we obtain the cross-species expression divergence D of a gene as the squared difference between the species mean levels. Cross-species differences in expression for a single gene are noisy and reflect the physiology of that gene, but averages over all or large classes of genes show a clear evolutionary pattern that can be compared with model expectations. In particular, the time-dependent expression divergence $\langle D_{ij} \rangle$, where i, j labels a given pair of species and angular brackets denote averages over genes, plays a central role in our analysis, as explained in Box 1. We define the rescaled divergence as

$$\Omega_{ij} = \frac{\langle D_{ij} \rangle}{D_0}, \qquad \text{(Equation 1)}$$

where the trait scale D_0 is defined such that $\Omega_{ij} \approx 1$ for neutral evolution in the limit of long divergence times (details of this definition are given in Experimental Procedures and Box 1). The evolution of these divergence measures depends only weakly on the effect distribution of expression QTL and on the amount of recombination between these loci, which is key to quantitative genetics approaches (Lynch and Hill, 1986; Leinonen et al., 2013; Nourmohammad et al., 2013a, 2013b; Held et al., 2014).

To obtain a genome-wide evolutionary picture of gene expression in *Drosophila*, we evaluate the aggregate time-dependent divergence for all genes and species in our dataset (Supplemental Experimental Procedures). Grouping the species into 6 clades, we obtain a consistent pattern of divergence $\Omega(\tau)$ as a function of divergence time τ (Figure 2). We can attribute this pattern to biological divergence of expression levels, because the species-specific design of microarrays suppresses technical errors that depend on evolutionary distance (Zhang et al., 2007). To test this prerequisite for evolutionary analysis, we compare the mean expression levels for specific

Box 1. Trait Evolution in a Fitness Seascape

FITNESS MODEL

The schematic shows the evolution of a quantitative trait in a single-peak fitness seascape (green curves). The distribution of trait values within a species (gray curves) changes over a macro-evolutionary period τ, which can be observed as cross-species divergence of the mean trait values $D(\tau)$ (gray arrow). The fitness seascape constrains trait values around a fitness peak by stabilizing selection, and evolutionary displacements of this peak generate directional selection (green arrow). The minimal fitness model has two parameters: the stabilizing strength c is proportional to the inverse square width of the fitness peak, and the driving rate υ measures the mean square displacement of the fitness peak per unit of evolutionary time (see Experimental Procedures and Supplemental Information). Lower plane: in a typical realization, the population mean trait (black line) follows the moving fitness optimum (green line) with delay and additional fluctuations.

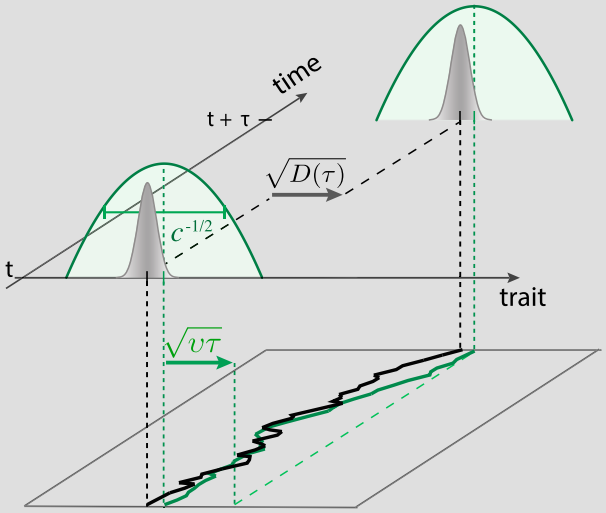

TIME-DEPENDENT DIVERGENCE

The rescaled mean square displacement $\Omega(\tau)$ is plotted against the rescaled divergence time τ. Neutral evolution (gray): $\Omega(\tau)$ reaches a saturation value of $\Omega_0 = 1$ with a relaxation time of $\tau_0 \sim 1$ (in units of the inverse mutation rate). Conservation (blue): in a single-peak fitness landscape, $\Omega(\tau)$ has a smaller saturation value, $\Omega_{stab} \sim 1/c$, which is reached faster than at neutrality, $\tau_{stab} \sim \Omega_{stab} < 1$. Adaptation (green): in a fluctuating fitness seascape, there is a linear surplus $\Omega_{ad}(\tau)$, which measures the amount of trait adaptation. We use the nonlinear relation between the trait divergence $\Omega(\tau)$ and the divergence time τ to infer the fitness parameters (c, υ).

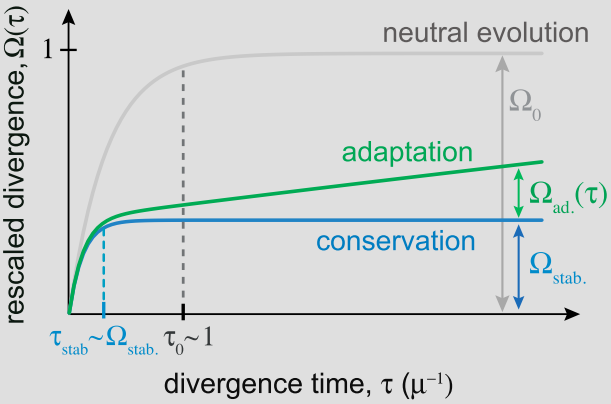

LINEAGE- AND GENE-SPECIFIC INFERENCE

Based on a joint probabilistic description of trait evolution and fitness fluctuations, we can infer the likelihood of the fitness parameters, stabilizing strength c and driving rate υ, for individual genes. The inference involves summing over all evolutionary histories of mean and optimal trait values across the phylogeny (black and green lines) that lead to the observed values $E_1, E_2, \ldots$, at the terminal nodes (shown here for three species). Over macro-evolutionary distances, this sum is dominated by the most parsimonious lineage-specific evolutionary history and can be evaluated analytically (see Experimental Procedures and Supplemental Information). The evolutionary histories on different branches mutually constrain each other because they are connected at the branch points (yellow diamonds).

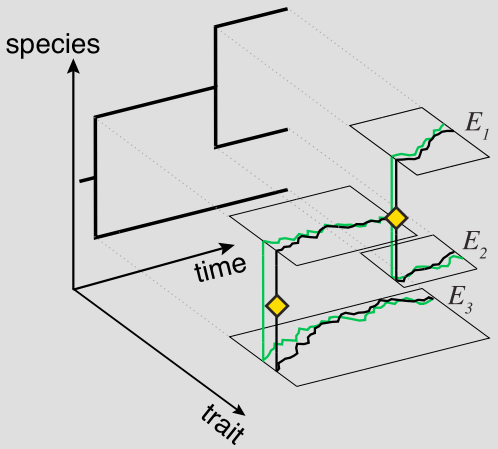

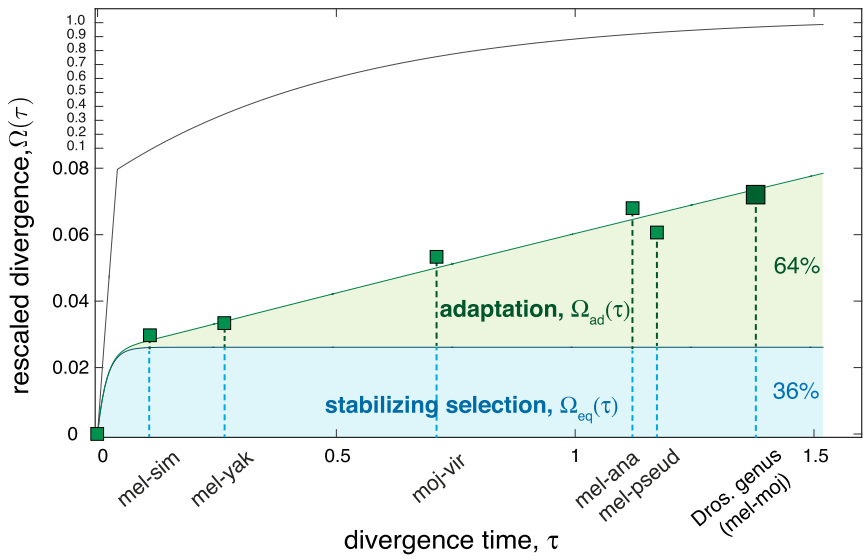

Figure 2. Adaptive Evolution of Gene Expression

The time-dependent divergence (rescaled) $\Omega(\tau)$ from all genes is plotted against the divergence time τ for six partial species clades (small squares) and for the entire *Drosophila* genus (large square). Species clades and divergence times (scaled by the rate of synonymous mutation) are defined by the phylogeny of the *Drosophila* genus (Figure 1). Trait divergence values are scaled by the asymptotic long-term limit under neutral evolution (see text and Experimental Procedures). These data are shown with theoretical curves $\Omega(\tau)$ under directional selection (green line), under stabilizing selection (blue line), and for neutral evolution (gray line). Inferred model parameters are stabilizing strength $c^* = 18.4$ and driving rate $v^* = 0.08$ (Box 1) (see Experimental Procedures and Supplemental Experimental Procedures). We infer a time-dependent adaptive component of the expression divergence $\Omega_{ad}(\tau)$ (green shaded area); the complementary component $\Omega_{eq}(\tau)$ (blue shaded area) is generated by genetic drift under stabilizing selection. Adaptation accounts for a fraction $\omega_{ad} = \Omega_{ad}/\Omega = 64\%$ of the expression divergence across the *Drosophila* genus ($\tau_{Dros.} = 1.4$). See Figure S3 for a comparison of the data to models of time-independent stabilizing selection (Bedford and Hartl, 2009); see also Figures S1, S2, and S4–S7.

gene classes across species. We find no distance-dependent differences, which provides strong evidence that our data are free of technical divergence caused by a species bias in probe sensitivity (Figure S1).

The rescaled expression divergence data in Figure 2 show macro-evolution of expression levels. The average expression divergence has two distinct molecular clocks: a rapid increase on timescales τ below the *D. melanogaster* (*D. mel*)-*D. simulans* (*D. sim*) divergence time is followed by a slower increase on larger timescales. This pattern is clearly incompatible with neutral evolution, where the rescaled divergence would follow a uniform linear pattern on short timescales and saturate to 1 on timescales given by the inverse point mutation rate (gray line in Figure 2, to be compared with the aggregate divergence plot in Box 1). The actual pattern shows stronger evolutionary constraint, which is clearly visible already within the *D. mel-D. sim-D. yakuba* (*D. yak*) clade: the species pair *D. mel-D. yak* has about twice the divergence time but only 1.2 times the expression divergence compared to the pair *D. mel-D. sim*. Hence, the characteristic constraint time is of the order $\tau_{mel-sim}$, about a factor of 10 shorter than the neutral saturation time. This pattern indicates evolution under substantial stabilizing selection, in qualitative agreement with previous studies (Supplemental Experimental Procedures) (Rifkin et al., 2003; Lemos et al., 2005; Bedford and Hartl, 2009) and with a standard Q_{ST}/F_{ST} analysis (Leinonen et al., 2013). However, the expression divergence increases with the divergence time throughout the *Drosophila* genus (green shaded area) and does not show evidence of saturation for larger values of divergence time τ. This observation is in accordance with a similar pattern of the expression divergence observed previously (Zhang et al., 2007) and is backed up by our probabilistic analysis reported later. In the following, we show that the increase of expression divergence beyond $\tau_{mel-sim}$ reflects adaptive evolution of gene expression over macro-evolutionary timescales, and we provide a parsimonious explanation for the separation of molecular clocks.

Fitness Model for Gene Expression

The inference of adaptation is based on a minimal dynamical model of selection: gene expression levels E evolve in a single-peak fitness seascape $f(E,t) = f^* - \text{const.} \times (E - E^*(t))^2$ (Nourmohammad et al., 2013a; Held et al., 2014). This model is illustrated in Box 1 and formally defined in Experimental Procedures. The fitness peak $E^*(t)$ for a given gene performs a random walk over macro-evolutionary periods, which maps continual changes of the optimal expression of that gene. Despite its simplicity, the seascape model combines two salient features of selection on gene expression: stabilizing selection generates evolutionary constraint, and directional selection drives long-term adaptive changes. These selection components are measured by two parameters: the stabilizing strength c, which is proportional to the inverse square width of the fitness peak, and the driving rate v, which measures the mean square displacement of the peak position $E^*(t)$ per unit of evolutionary time. The fitness peak value f^* is arbitrary, because only fitness differences between individuals matter for the evolution of a species.

The fitness seascape model captures distinct selective causes of adaptive evolution. Long-term environmental shifts can lead to changes in the optimal expression levels that accumulate over macro-evolutionary periods. The co-evolution of genes in networks acts in a similar way: changes in the expression of one gene generate time-dependent selection on the expression of functionally correlated genes. This time dependence broadly describes cross-gene epistasis in regulatory and metabolic pathways. The seascape model is not concerned with individual environmental shifts or epistatic changes; it describes the evolutionary system biology of cumulative effects over macro-evolutionary periods and over groups of genes. These effects can

be inferred from our kind of dataset and give rise to a random walk model for fitness peak positions $E^*(t)$. Later, we extend this model to include larger, punctuated shifts of fitness peaks.

Inference of Adaptive Evolution

Time-dependent selection generates complex evolutionary dynamics of expression levels for a given gene. The top diagram of Box 1 shows a typical pattern: the population mean level follows the fitness peak displacements with some delay; additional deviations of mean and optimal trait value are generated by genetic drift. The fitness seascape model provides a simple conceptual and computational basis to infer these dynamics. The simplest inference scheme is based on aggregate time-dependent expression divergence data; a probabilistic extension to individual genes is discussed later. Box 1 shows the analytical form of the rescaled trait divergence $\Omega(\tau)$ in a fitness seascape with positive stabilizing strength and driving rate ($c>0$, $\upsilon>0$; green solid line); the corresponding form $\Omega_{\rm eq}(\tau)$ in a fitness landscape of the same stabilizing strength and zero driving rate ($c>0$, $\upsilon=0$; blue solid line) reaches the saturation value $\Omega_{\rm stab}$ (Nourmohammad et al., 2013a; Held et al., 2014). The saturation time is inversely proportional to the stabilizing strength $\tau_{\rm stab}\sim\Omega_{\rm stab}\sim 1/c$ and is shorter than expected from neutral evolution $\tau\sim 1$ (gray solid line). The resulting decomposition

$$\Omega(\tau)=\Omega_{\rm eq}(\tau)+\Omega_{\rm ad}(\tau) \qquad \text{(Equation 2)}$$

determines the adaptive fraction $\omega_{\rm ad}(\tau)=\Omega_{\rm ad}(\tau)/\Omega(\tau)=\langle D_{\rm ad}(\tau)\rangle/\langle D(\tau)\rangle$ of the trait divergence, which is driven by directional selection; the complementary fraction $1-\omega_{\rm ad}(\tau)$ is generated by genetic drift under stabilizing selection. In the linear regime $\Omega(\tau)\approx\Omega_{\rm stab}+\Omega_{\rm ad}(\tau)$, which covers all species clades in this dataset, the fitted amplitudes provide simple estimates of the selection parameters (Held et al., 2014):

$$c\approx\frac{2}{\Omega_{\rm stab}},\quad \upsilon\approx\frac{2\Omega_{\rm ad}(\tau)}{\tau}. \qquad \text{(Equation 3)}$$

Here we determine these parameters, together with the trait scale D_0, by a maximally conservative inference procedure, which produces the smallest value of stabilizing strength c compatible with the data (Experimental Procedures).

How much adaptation is in the evolutionary process? This can be measured by the fitness flux Φ, which is the cumulative fitness gain through adaptive changes over an evolutionary period (Mustonen and Lässig, 2007, 2010; Held et al., 2014). For a gene with evolving mean expression level $\Gamma(t)$, the fitness flux at a given time t is defined as the rate $d\Gamma(t)/dt$ of expression change multiplied by the fitness gradient $\partial F(\Gamma,t)/\partial\Gamma$, where $F(\Gamma,t)$ is the mean fitness of the population at time t (Supplemental Experimental Procedures). Positive fitness flux under time-dependent selection does not imply a net gain in fitness, because fitness gains through adaptation can be offset by losses through displacements of the fitness peak. We can compare these dynamics to walking on an escalator that moves in the opposite direction. The quantity Φ corresponds to the walker's total number of uphill steps on the escalator but is unrelated to an absolute height gain. In the seascape model, the fitness flux is proportional to the driving rate υ and to the stabilizing strength c, because a population under stronger selection follows the fitness peak more closely and accumulates more adaptation. Hence, the cumulative fitness flux Φ over an evolutionary period τ has the expectation value $\langle 2N\Phi(\tau)\rangle=2\,c\upsilon\,\tau$ (scaled by the effective population size N) (Held et al., 2014). Equation 3 establishes a simple relation between fitness flux and the adaptive part of the expression divergence:

$$\langle 2N\Phi(\tau)\rangle\approx\frac{2\omega_{\rm ad}(\tau)}{1-\omega_{\rm ad}(\tau)}. \qquad \text{(Equation 4)}$$

Thus, the time-dependent pattern of expression divergence discriminates directional selection in a genuine fitness seascape from purely stabilizing selection in a static fitness landscape. The joint inference of these selection components provides a more powerful signal of adaptation than Q_{ST}/F_{ST} analysis (Leinonen et al., 2013), which would infer only stabilizing selection from these data. In Supplemental Experimental Procedures, we discuss in detail the relationship between the test for selection based on trait divergence and other trait-based selection tests: the Q_{ST}/F_{ST} test (Leinonen et al., 2013), Ornstein-Uhlenbeck models (Hansen, 1997; Bedford and Hartl, 2009), and the McDonald-Kreitman test (McDonald and Kreitman, 1991).

Fitness Seascape of *Drosophila* Gene Expression

We first use the aggregate time-dependent divergence data to infer a gene-averaged fitness seascape of expression levels in *Drosophila* (Figure 2). The least-square fitted seascape model (green line) contains stabilizing and directional selection, as illustrated in the center plot of Box 1. This model explains the observed pattern $\Omega(\tau)$: the evolutionary constraint between neighboring species (here *D. mel*, *D. sim*, and *D. yak*) is caused by stabilizing selection, and the approximately linear long-term increase signals adaptation.

Our inference also shows that stabilizing selection alone cannot explain the *Drosophila* expression data. In a static fitness landscape with substantial stabilizing strength, genetic drift generates a rapidly saturating pattern of $D(\tau)$ that is not observed in the data (Figure S3). A previous study of this dataset suggests a pattern with slow saturation on timescales on the order of the *Drosophila* genus divergence time (Bedford and Hartl, 2009); such a pattern would imply weak stabilizing selection $(c<1)$ and near-neutral evolution of gene expression levels (see Supplemental Experimental Procedures for a detailed discussion). Compared to the seascape model, the weak-selection landscape model provides a suboptimal fit to the observed $D(\tau)$ data (Figure S3). This ranking of models is confirmed and quantified by the probabilistic analysis.

Probabilistic Inference of Adaptively Regulated Genes

Next, we extend the inference of selection to the noisy patterns of individual genes. Using probabilistic extension of the selection test, we obtain gene-specific posterior likelihood distributions of stabilizing strength and fitness flux $Q(c,\Phi)$ (Box 1) (Experimental Procedures). Maximizing this function allows us to infer, for each gene, the most likely values of stabilizing strength c and fitness flux Φ (or, equivalently, of c and υ) given its observed expression

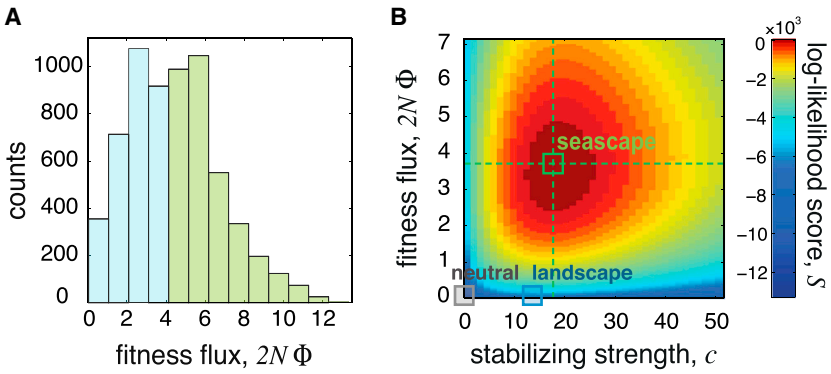

Figure 3. Probabilistic Inference of Adaptive Gene Expression

(A) Distribution of maximum-likelihood values of the scaled cumulative fitness flux, $2N\Phi$, inferred for individual genes (see Experimental Procedures and Supplemental Experimental Procedures). Our inference classifies 54% of all genes as adaptively regulated ($2N\Phi > 4$, green shaded part of the distribution).

(B) Bayesian inference of fitness models. The posterior log-likelihood score $S(c, \Phi)$ favors the optimal seascape model ($c^* = 18.4$, $2N\Phi^* = 3.8$; green square) over the best landscape model ($c^*_{eq} = 16$, $\Phi = 0$; blue square) and the neutral model ($c = 0$, $\Phi = 0$; gray square).

See also Figures S1, S2, S6, and S7.

values in 7 *Drosophila* species on the phylogeny of Figure 1 (see also Box 1).

This analysis shows again the dominant role of adaptation in gene expression: for 54% of all genes, we infer a significant maximum-likelihood fitness flux Φ across the *Drosophila* genus; we classify these genes as adaptively regulated (Table S1). Figure 3A shows the distribution of maximum-likelihood values of the fitness flux for individual genes, which determines the inferred clade-specific fraction of adaptive expression divergence (Table 1). This fraction $\omega_{ad}(\tau)$ increases with clade divergence time, in accordance with the aggregate data of Figure 2. Between *D. mel* and *D. sim*, which diverged about 2–3 mya, 92% of the expression divergence can be attributed to genetic drift under stabilizing selection. Across the entire *Drosophila* genus, which had its last common ancestor about 40 mya ago, we infer 64% of the expression divergence to be adaptive.

The Bayesian scheme also allows us to quantify the overall statistical significance of our selection inference. In Figure 3B, we plot the cumulative log-likelihood score for all genes as a function of stabilizing strength c and cumulative fitness flux Φ. As shown by a log-likelihood test, the global maximum-likelihood seascape model is strongly favored over the maximum-likelihood landscape model ($P < 10^{-3600}$) and over neutral evolution ($P < 10^{-5400}$) (see Equation 35 in Supplemental Experimental Procedures). This analysis rejects neutral evolution and evolution under static stabilizing selection in a robust way: it does not require model assumptions on the adaptive dynamics, and the ranking of models is stable under alternate evaluation of species divergence times (Figure S2). We conclude that the long-term increase of expression divergence beyond the *D. mel-D. sim* divergence time, as observed in Figure 2, is a statistically significant signal of adaptive evolution.

Drift and Adaptation Follow Distinct Molecular Clocks

The fitness seascape model interprets the two molecular clocks observed in gene expression divergence in terms of distinct evolutionary forces: the rapid short-term increase is caused by genetic drift, whereas the slower long-term increase is caused by adaptation. Because genetic drift and adaptation differ in tempo, the relative contribution of adaptation to expression divergence depends on evolutionary time: the adaptive part is small for the youngest species clades, but adaptation becomes dominant across the entire *Drosophila* genus (green shaded area in Figure 2). This nonlinearity is a specific evolutionary feature of quantitative traits with a complex molecular basis, which can have individual loci under weak selection (Sunyaev and Roth, 2013). Substitutions at these loci generate predominantly diffusive divergence of expression on short timescales ($\tau < \tau_{stab}$); this pattern is modified by stabilizing and directional selection on longer timescales.

The existence of two molecular clocks has an immediate consequence: the power of inference methods for trait adaptation increases with evolutionary time span. Quantitative genetics studies over short divergence times cannot distinguish neutral evolution from evolution under selection, because the divergence pattern is dominated by the diffusive molecular clock in both cases (Box 1). For example, the observation of drift-dominated behavior in primates (Khaitovich et al., 2004) is consistent with neutral evolution but cannot exclude stabilizing or directional selection. Thus, it is compatible with the signal of adaptive evolution based on expression QTLs in humans (Fraser, 2013). In contrast, the data from the 7 *Drosophila* species spans both short and long divergence times and displays two molecular clocks. This divergence pattern is no longer consistent with neutral evolution and is indicative of macro-evolutionary adaptation of gene expression in *Drosophila*.

Testing Alternative Evolutionary Scenarios

The minimal seascape model explains the pattern of gene expression divergence across the *Drosophila* genus in a parsimonious way. But are there equally parsimonious alternative modes of selection or demography that are consistent with the data? To assess the specificity and robustness of the seascape-based inference, we characterize the statistics of gene expression levels in a number of alternative modes of evolution by analytical approximations and simulations, and we compare the results to the *Drosophila* data.

First, demographic effects may increase or decrease the effective population size in a specific lineage, which affects the stabilizing strength c for all genes. As shown in Figure S4, lineage-specific changes in effective population size that persist over sufficiently long evolutionary periods can be traced in the aggregate time-dependent divergence $\Omega(\tau)$. Such effects are not observed in our data, which suggests that long-term demographic effects do not play a dominant role in the evolution of *Drosophila* gene expression levels (Figure S4). This result does not exclude short-term changes of population size, which

Table 1. Selection Parameters and Amount of Adaptation

Gene classes (gene number)	c^*	$2N\Phi^*$	*D. mel-D. sim*	*D. mel-D. yak*	*D. vir-D. moj*	*D. mel-D. ana*	*D. mel-D. pse*	*Dros.* (*D. mel-D. moj*)
					ω_{ad} (%)			α (%)
All genes (6,332)	18.4	3.8	7	23	48	59	61	64	54
Broad codon usage (1,176)	15.6	3.9	9	25	49	61	62	66	57
Narrow codon usage (501)	18.0	2.4	5	15	36	48	49	53	18
High expression (553)	14.3	1.7	1	8	27	39	40	44	0

Dros., *Drosophila* genus; c^*, maximum-likelihood stabilizing strength; $2N\Phi^*$, maximum-likelihood fitness flux; ω_{ad}, clade-dependent adaptive fraction of the gene expression divergence; α, fraction of adaptively regulated genes across the *Drosophila* genus, given by the condition $2N\Phi^{\alpha} > 4$.

occurred, for example, in the evolution of the *D. mel* lineage (Lachaise et al., 1988). Such changes can be traced in sequence polymorphism spectra (Glinka et al., 2003; Haddrill et al., 2005; Stephan and Li, 2007; Thornton et al., 2007), but they have only minor effects on gene expression levels (Figure S4).

Next, we ask whether the *Drosophila* data can be explained by lineage- and gene-specific relaxation of stabilizing selection. We consider a specific non-adaptive mode of expression changes: functional genes evolve under stabilizing selection in a static fitness landscape, but individual genes can (partially) lose function at a given point in their evolutionary history, which relaxes selection on their expression. We model loss of function as stochastic events occurring at a small rate, independently for each gene and on each lineage. This model produces a divergence function $\Omega(\tau)$ with a long-term nonlinearity that is not seen in the Ω data (Figure S5). The most direct way to discriminate between relaxation of selection and adaptive evolution is to use a directional bias: most functional genes are upregulated by stabilizing selection (a similar bias has been exploited in expression QTL studies) (Fraser et al., 2010; Fraser, 2011, 2013). Hence, in the loss-of-function mode, a comparison of expression levels for a given gene would show small cross-species differences at higher expression levels (i.e., between the lineages with a functional gene), together with large deviations at lower levels (i.e., in the lineages with lost gene function). Accordingly, the distribution of expression divergence values for a given species pair would show a broad tail generated by the loss events (Figure S5). These features are not observed in our data, indicating that relaxed stabilizing selection alone cannot explain the evolution of *Drosophila* expression levels (Figure S5). Loss of gene function does happen in our phylogeny, but affected genes will often lose expression altogether and hence will be suppressed in our dataset.

We also compare the *Drosophila* data with alternative models of adaptive evolution. For example, individual genes can undergo a (partial) neo-functionalization that requires a major change in their expression. We describe this mode of evolution by a punctuated fitness seascape, in which large shifts of the peak position are stochastic events occurring at a small rate (Held et al., 2014). This process produces an aggregate divergence function $\Omega(\tau)$ that is compatible with the data, but a broad tail in the distribution of expression divergence values is not observed (Figure S5). We conclude that gradual but continual changes in optimal levels, as described by our minimal model, are the dominant evolutionary force driving the adaptation of gene expression in *Drosophila*.

Functional Determinants of Selection

By applying our inference to specific classes of genes, we can get a more detailed view on adaptation of gene expression in *Drosophila.* First, we observe a strong correlation between codon usage and adaptation: genes with specific codons show strongly reduced adaptive expression divergence and lower average fitness flux than genes with broad codon usage (Figure 4; Table 1). Specific codon usage is known to be prevalent in highly expressed genes (Ikemura, 1985); consistently, we find stronger conservation of expression and lower levels of fitness flux in this class (Table 1). Different codons for the same amino acid differ in their efficiency of translation (Ikemura, 1985; Shields et al., 1988), which implies that genes with broad codon usage have a higher potential for adaptive changes at the post-transcriptional level. Here we find stronger adaptation at the mRNA level in this gene class, which suggests a two-tier mode of evolution: adaptive mRNA changes lay the ground on which coherent adaptive tuning of protein levels can build.

At the same time, we find no significant correlation between fitness flux for expression changes and adaptation of the amino acid sequence, as measured by a McDonald-Kreitman test (Figure S6) (McDonald and Kreitman, 1991). This decoupling makes sense, because expression changes of a gene are caused by *cis*- and *trans*-regulatory sequence changes but do not require evolution of its coding sequence. At the broad level of analysis afforded by our dataset, we conclude that for a given gene, expression level and coding sequence evolve independently to a large degree. For a metabolite or a transcription factor, adaptive changes of its cellular concentration are often coupled with conservation of its function.

Our gene-specific inference can be used to detect functional gene classes associated with adaptive evolution of regulation. A full ranking of gene classes by enrichment in adaptively regulated genes with associated p values is reported in Table S1. Gene functions associated with enhanced adaptation of expression include sensory perception, regulation, neural maturation, regulation of growth, aging, and morphology. Adaptively regulated functions also include response to UV radiation, which has been identified as an important climate-mediated trait in humans (Hancock et al., 2011; Fraser, 2013). Adaptive evolution of

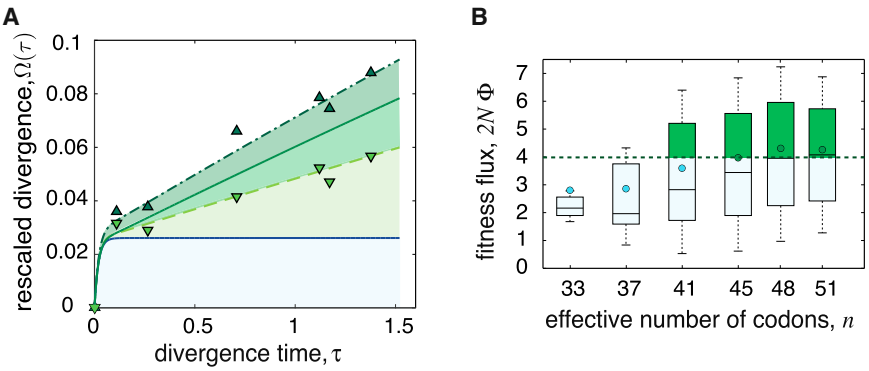

Figure 4. Adaptation of Gene Expression Depends on Codon Usage Bias

(A) The aggregate time-dependent divergence $\Omega(\tau)$ for genes with broad codon usage ($\triangle$) and for genes with specific codon usage ($\triangledown$) is shown, together with theoretical curves under directional selection (dashed and dashed-dotted lines); the theoretical curve inferred for all genes is shown for comparison (solid line; cf. Figure 2). Codon usage is measured by the effective number of codons (Supplemental Experimental Procedures) (Wright, 1990); inferred model parameters are listed in Table 1.

(B) The distribution of the cumulative fitness flux $2N\Phi$ is plotted against the effective number of codons n (circle, average; line, median; box, 50% around median; bars, 70% around median) (Supplemental Experimental Procedures) (Wright, 1990). See also Figures S1, S2, S4, S5, and S7.

genes related to growth, regulation, and morphology has been previously inferred by expression QTL and comparative studies of gene regulation in other species (Fraser et al., 2011; Fraser, 2011; Romero et al., 2012). Here we identify these categories from a quantitative, system-wide scan for adaptively regulated genes. This points to the power of our phenotype-based inference scheme, which is not confounded by the combinatorial complexity of *cis*-regulatory sequence in higher eukaryotes.

Sex-Specific Evolution of Expression

We test the role of expression differentiation between male and female samples for adaptive evolution across the *Drosophila* genus. The sex specificity of a given gene (Zhang et al., 2007), defined as the difference between its male and female expression level $E_{mf} = E_m - E_f$, is a distinct trait whose evolutionary pattern can be analyzed by our method. We can distinguish two modes of evolution: conservation of sex specificity maintained by stabilizing selection and sex-specific adaptation of expression (Figure 5A). Most genes of our dataset have well-conserved and often small sex specificity; these genes evolve their expression levels coherently between males and females (Zhang et al., 2007). The remaining 19% of the genes have a significant cumulative fitness flux Φ_{mf} of their specificity trait; we classify them as undergoing sex-specific adaptation of expression in the *Drosophila* genus. These genes cover all four chromosomes of the *Drosophila* genome.

Gene functions associated with sex-specific adaptation of expression include regulation of translation, reproduction, post-mating behavior, and (immune) response to biotic stimuli (Table S2). To understand the distribution of these adaptive processes between sexes, we apply our inference to classes of genes with different species-averaged sex bias of expression (Assis et al., 2012). For male-biased genes, the aggregate divergence Ω_{mf} signals substantial sex-specific adaptation (Figure 5B). Consistently, fitness flux Φ_{mf} is strongly enhanced in genes that are predominantly expressed in males (Figure 5C). Fitness flux is lower in other classes, including genes expressed predominantly in females.

Altogether, we find a remarkable evolutionary asymmetry between sexes: male bias in expression is associated with adaptive evolution of expression (orange shaded areas in Figures 5B and 5C), whereas female bias in expression is under weaker directional selection and primarily reflects conserved physiological differences between male and female organisms. This result complements a previously observed evolutionary asymmetry at the sequence level: genes with male-biased expression show increased amino acid divergence (Zhang et al., 2007). As suggested by a McDonald-Kreitman test, this increase can be associated with adaptive evolution of gene function (Figure S6).

DISCUSSION

We have shown that adaptive regulation accounts for most of the macro-evolutionary divergence in gene expression across the *Drosophila* genus. Genes differ considerably in the amount of adaptation, depending on their codon usage, sexual differentiation, and functional class. These results provide evidence for system-wide adaptation of gene regulation in *Drosophila* at the primary level of transcription, notwithstanding further evolutionary complexities at the level of translation (Romero et al., 2012; Artieri and Fraser, 2014). It remains to be seen whether a similar prevalence of adaptation in the evolution of expression will be found in different species.

Our inference of adaptation exploits the complex dependence of the expression divergence on the evolutionary distance between species. It reflects two fundamental evolutionary features of quantitative traits. First, such traits generate a divergence pattern with two distinct molecular clocks: at a short evolutionary distance, the divergence is always near the expected value under neutrality; at a longer distance, it depends jointly on stabilizing and directional selection (Figure 2; Box 1). This feature reconciles seemingly contradictory results of previous studies: analysis of closely related species produces a signal of neutral evolution (Khaitovich et al., 2004, 2005), whereas evolutionary constraint becomes apparent for more distant species (Rifkin et al., 2003; Lemos et al., 2005; Rifkin et al., 2005; Gilad et al., 2006; Bedford and Hartl, 2009; Romero et al., 2012). Second, the phenotypic evolution of gene expression decouples from details of its genetic basis. This explains why we find overall strong selection on gene expression levels even though selection on

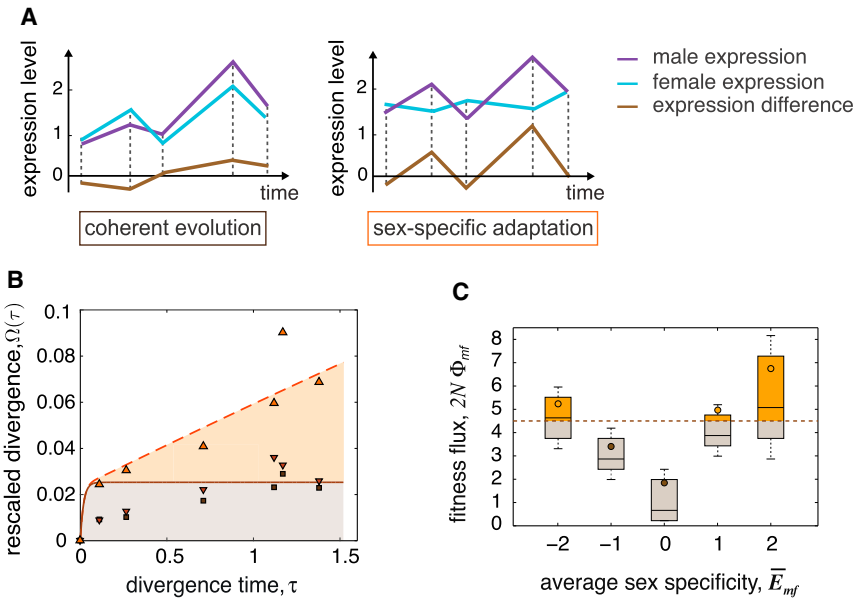

Figure 5. Sex-Specific Evolution of Gene Expression

(A) Schematic showing conservation of sex specificity (left panel) versus sex-specific adaptation of expression (right panel). The sex-specificity trait (brown line) is defined as the difference between male and female expression levels (purple and blue lines). The schematics show all three lines as functions of evolutionary time.

(B) The time-dependent divergence of the sex-specificity trait Ω_{mf} for all genes (□), genes with male-biased expression (△), and genes with female-biased expression (▽) is shown, together with theoretical curves under directional selection.

(C) The distribution of the cumulative fitness flux for the sex-specificity trait $2N\Phi_{mf}$ is plotted against the species-averaged sex specificity $\overline{E}_{mf}$ (circle, average; line, median; box, 50% around median; bars, 70% around median) (Supplemental Experimental Procedures). Sex-specific adaptation ($2N\Phi_{mf} > 4.5$, orange shaded part) occurs predominantly in male-biased genes.

See also Figures S1 and S4–S7.

individual QTL is often weak (Sunyaev and Roth, 2013). The probabilistic extension of our inference scheme, which is based on gene-specific expression divergence, identifies functional gene classes associated with adaptive evolution of regulation.

The selection model underlying our analysis is a single-peak fitness seascape, which contains components of stabilizing and directional selection on a quantitative trait (Box 1). These components are well-established notions of quantitative genetics on micro-evolutionary timescales. Each of them can provide a snapshot of the predominant selection pressure in a population. However, the description of selection remains incomplete as a description of selection over macro-evolutionary periods. If selection on a trait is directional at a given evolutionary time, will that selection relax after the trait value has significantly adapted in the direction of selection? If selection is stabilizing, can we assume the optimal trait value will remain invariant in the context of a different species? To address these questions, we need a conceptual and quantitative synthesis of stabilizing and directional selection. The single-peak seascape model arguably provides the simplest such synthesis. It also provides a simple picture of continual adaptation over macro-evolutionary periods: a species follows a moving fitness peak, and this process generates positive fitness flux but no net increase in fitness.

Our method of selection inference can be applied to a spectrum of molecular quantitative traits with a complex genetic basis, provided that comparative data from multiple, sufficiently diverged species are available. Such traits include genome-wide protein levels, protein-DNA binding interactions, and enzymatic activities. For most of these traits, we have only partial knowledge of the underlying genetic loci and their effects on trait and fitness. Our method complements QTL studies and opens a way to infer quantitative phenotype-fitness maps at the systems level.

EXPERIMENTAL PROCEDURES

Sequence Data and Evolutionary Tree

A synonymous genome sequence is used to estimate the species divergence times τ_{ij} (scaled in units of the inverse point mutation rate μ^{-1} (Drosophila 12 Genomes Consortium et al., 2007). The resulting phylogeny (Drosophila 12 Genomes Consortium et al., 2007) is shown in Figure 1, where we also compare the divergence times τ_{ij} with divergence measures based on amino acid distances.

Expression Data and Primary Analysis

We use genome-wide expression data from 7 *Drosophila* species (*D. melanogaster* [*D. mel*], *D. simulans* [*D. sim*], *D. yakuba* [*D. yak*], *D. ananassae* [*D. ana*], *D. pseudoobscura* [*D. pse*], *D. virilis* [*D. vir*], and *D. mojavensis* [*D. moj*]), obtained in Zhang et al. (2007) (GEO: GSE6640). These data contain mRNA intensity measurements for a number of biological replicates from adult (5–7 days post-eclosion) males and females in each species. For quality assessment, a number of technical replicates were obtained for each biological replicate. Moreover, specific microarray platforms were designed for each of these species, which allows for a reliable comparison of expression levels across species (Figure S1) (Zhang et al., 2007). We restrict the analysis to the 6,332 genes that have unambiguous one-to-one orthologs across all lines and are tested by at least four probes in each microarray platform (see Supplemental Information for details).

The expression levels $E^{\alpha}_{i,s,\kappa}$ are labeled by gene α, species i, sex s, and biological replicates κ. The levels are transformed to mean 0 and cross-gene variance 1 for each replicate (Z-transformation of microarrays) (Quackenbush, 2002). In the Supplemental Experimental Procedures, we show that this transformation accurately captures evolutionary information and that our results are robust under quantitative details of the transformation (Figure S1). Furthermore, the assays do not generate a spurious signal of expression divergence across species (Figure S1). For a given gene α, we estimate the variance across biological replicates δ^{α}_{i} and genetic mean Γ^{α}_{i} in each species and the divergence $D^{\alpha}_{ij} = (\Gamma^{\alpha}_{i} - \Gamma^{\alpha}_{j})^2$ between any two species i, j. These divergence data inform our primary inference of adaptation. For each pair of species, we evaluate the aggregate divergence $\langle D_{ij} \rangle$ and the rescaled divergence $\langle \Omega_{ij} \rangle$ given by Equation 1, using a trait scale D_0 obtained by our model fit (described later). For each clade $\mathcal{C}$ in our phylogeny, we obtain the aggregate data $(\tau_{\mathcal{C}}, \Omega_{\mathcal{C}})$ shown in Figures 2, 4A, and 5B by averaging τ_{ij} and Ω_{ij} over all

pairs of species $i,j \in \mathcal{C}$ that are connected via the root of the clade. Unlike pairwise divergence between species, clade-specific divergence data allow unbiased error analysis and model ranking, because they are only weakly correlated through the structure of the phylogeny (Figure 1).

Inference of Selection

The minimal fitness seascape for a given gene takes the form

$$f(E,t) = f^* - \frac{c}{2NE_0^2}(E - E^*(t))^2,$$

where the optimal trait value $E^*(t)$ performs an Ornstein-Uhlenbeck process with mean square displacement υE_0^2 per unit μ^{-1} of evolutionary time (Box 1); E_0^2 is the average genetic variation of expression in the long-term limit of neutral evolution (Nourmohammad et al., 2013b).

We use the time dependence of the clade-specific aggregate expression divergence $(\tau_C, \langle D_C(\tau)\rangle)$ to infer the fitness parameters of stabilizing strength c and driving rate υ. We treat the trait scale D_0 as an additional fit parameter and assume that the saturation due to stabilizing selection occurs at the latest possible time (i.e., for the largest Ω_{stab}) consistent with the data, resulting in a best model with conservative estimates of stabilizing strength c. This assumption is necessary because the resolution of the data on short evolutionary timescales is bounded by the *D. mel-D. sim* divergence. Using this procedure, we infer a global fitness seascape with parameters $(c^* = 18.4,\ \upsilon^* = 0.08)$ and a resulting average fitness flux $2N\Phi^* = 3.8$ per gene across the *Drosophila* genus $(\tau_{\text{Dros.}} = 1.4)$ (Figure 2). The fitness flux is independent of the trait scale D_0 and hence of the preceding assumption. Moreover, we use the trait scale D_0 and the neutral sequence diversity π_0 determined from synonymous polymorphisms (Begun et al., 2007) to estimate the expected aggregate trait diversity within a given species $\langle\Delta\rangle \sim \pi_0 D_0$ (Supplemental Experimental Procedures). This estimate of $\langle\Delta\rangle$ determines the sampling error of the observed expression divergence D (Figure 2 shows error-corrected divergence data). Conversely, the trait scale D_0 can be inferred directly from data of $\langle\Delta\rangle$ (Supplemental Experimental Procedures), but such data are not available for all species in the present set.

Control fits of the same data to equilibrium models, including the well-known Ornstein-Uhlenbeck dynamics for the population mean trait (Hansen, 1997; Bedford and Hartl, 2009), are shown in Figure S3. To account for the expression noise due to the limited number of biological replicates in each species, we use a probabilistic extension of this test. We evaluate the Bayesian posterior probability distribution for the stabilizing strength and fitness flux in individual genes $Q(c,\Phi \mid \mathbf{E}^\alpha)$, given their sample mean data $\mathbf{E}^\alpha = (E_1^\alpha, \ldots, E_7^\alpha)$. This produces gene-specific expectation values c^α and Φ^α (Figures 3A, 4B, and 5C). This method uses gene-specific trait scales D_0, which account for differences in mutational variance between genes. We use a conservative condition on fitness flux $2N\Phi^\alpha > 4$ to infer adaptively regulated genes (Table S1). The cumulative log-likelihood score $S(c,\Phi) = \sum_\alpha \log Q(c,\Phi \mid \mathbf{E}^\alpha)$ quantifies the statistical significance of our inference (Figure 3B).

Analysis of Alternative Evolutionary Scenarios

To test for lineage-specific demographic effects, we compare the aggregate rescaled divergence $\Omega = \langle D(\tau)\rangle / D_0$ data to theoretical functions $\Omega(\tau,\tau_i)$ computed for an alternative model with a change in effective population size on the phylogenetic branch of species i (Figure S4). We also examine two alternative selection scenarios: relaxed stabilizing selection by partial loss of function (c^α switches to a reduced value with rate γ) and punctuated fitness peak shifts ($E^{*\alpha}$ jumps by an amount on the order of E_0 with a rate on the order of $\upsilon\mu$) (Figure S5). The observed distributions of cross-species expression differences are consistent with the minimal seascape model but at variance with both alternative models (Figure S5).

Analysis of Specific Gene Classes

To infer sex-specific evolution, we define specificity traits as differences between male and female expression levels $E_{mf,i}^\alpha = E_{m,i}^\alpha - E_{f,i}^\alpha$ for each gene (Zhang et al., 2007). Genes with sex-specific adaptive evolution of expression are identified by a condition on the cumulative fitness flux for the specificity trait $2N\Phi_{mf}^\alpha > 4.5$ (Table S2). Genes with male- and female-biased expression are identified using the results of Assis et al. (2012).

Simulation Tests

We simulate Fisher-Wright evolution to validate our probabilistic inference scheme and to establish its robustness under trait epistasis (Figure S7).

SUPPLEMENTAL INFORMATION

Supplemental Information includes Supplemental Experimental Procedures, seven figures, and two tables and can be found with this article online at http://dx.doi.org/10.1016/j.celrep.2017.07.033.

AUTHOR CONTRIBUTIONS

A.N., J.R., T.H., V.K., J.B., and M.L. designed the research and analyzed the data. A.N., T.H., and M.L. wrote the article.

ACKNOWLEDGMENTS

We acknowledge discussions with P. Andolfatto, N. Barton, A. Beyer, H. Fraser, M. Łuksza, L.B. Oliver, J. Plotkin, S. Schiffels, P. Shah, and D. Sturgill. This work has been supported by the James S. McDonnell Foundation (A.N.), U.S. National Science Foundation grant PHY1305525 (A.N.), and Deutsche Forschungsgemeinschaft grant SFB 680. We acknowledge the U.S. National Science Foundation grant PHY1125915 to the Kavli Institute of Theoretical Physics (UCSB), where part of this work was performed.

Received: September 6, 2016
Revised: April 15, 2017
Accepted: July 13, 2017
Published: August 8, 2017

REFERENCES

Andolfatto, P. (2005). Adaptive evolution of non-coding DNA in *Drosophila*. Nature *437*, 1149–1152.

Artieri, C.G., and Fraser, H.B. (2014). Evolution at two levels of gene expression in yeast. Genome Res. *24*, 411–421.

Assis, R., Zhou, Q., and Bachtrog, D. (2012). Sex-biased transcriptome evolution in *Drosophila*. Genome Biol. Evol. *4*, 1189–1200.

Bedford, T., and Hartl, D.L. (2009). Optimization of gene expression by natural selection. Proc. Natl. Acad. Sci. USA *106*, 1133–1138.

Begun, D.J., Holloway, A.K., Stevens, K., Hillier, L.W., Poh, Y.P., Hahn, M.W., Nista, P.M., Jones, C.D., Kern, A.D., Dewey, C.N., et al. (2007). Population genomics: whole-genome analysis of polymorphism and divergence in *Drosophila simulans*. PLoS Biol. *5*, e310.

Blekhman, R., Oshlack, A., Chabot, A.E., Smyth, G.K., and Gilad, Y. (2008). Gene regulation in primates evolves under tissue-specific selection pressures. PLoS Genet. *4*, e1000271.

Brawand, D., Soumillon, M., Necsulea, A., Julien, P., Csárdi, G., Harrigan, P., Weier, M., Liechti, A., Aximu-Petri, A., Kircher, M., et al. (2011). The evolution of gene expression levels in mammalian organs. Nature *478*, 343–348.

Bullard, J.H., Mostovoy, Y., Dudoit, S., and Brem, R.B. (2010). Polygenic and directional regulatory evolution across pathways in *Saccharomyces*. Proc. Natl. Acad. Sci. USA *107*, 5058–5063.

Coolon, J.D., McManus, C.J., Stevenson, K.R., Graveley, B.R., and Wittkopp, P.J. (2014). Tempo and mode of regulatory evolution in *Drosophila*. Genome Res. *24*, 797–808.

Drosophila 12 Genomes Consortium, Clark, A., Eisen, M., Smith, D., Bergman, C., Oliver, B., Markow, T., Kaufman, T., Kellis, M., Gelbart, W., Iyer, V., et al. (2007). Evolution of genes and genomes on the *Drosophila* phylogeny. Nature *450*, 203–218.

Fraser, H.B. (2011). Genome-wide approaches to the study of adaptive gene expression evolution: systematic studies of evolutionary adaptations involving gene expression will allow many fundamental questions in evolutionary biology to be addressed. BioEssays *33*, 469–477.

Fraser, H.B. (2013). Gene expression drives local adaptation in humans. Genome Res. *23*, 1089–1096.

Fraser, H.B., Moses, A.M., and Schadt, E.E. (2010). Evidence for widespread adaptive evolution of gene expression in budding yeast. Proc. Natl. Acad. Sci. USA *107*, 2977–2982.

Fraser, H.B., Babak, T., Tsang, J., Zhou, Y., Zhang, B., Mehrabian, M., and Schadt, E.E. (2011). Systematic detection of polygenic *cis*-regulatory evolution. PLoS Genet. *7*, e1002023.

Genissel, A., McIntyre, L.M., Wayne, M.L., and Nuzhdin, S.V. (2008). *Cis* and *trans* regulatory effects contribute to natural variation in transcriptome of *Drosophila melanogaster*. Mol. Biol. Evol. *25*, 101–110.

Gilad, Y., Oshlack, A., Smyth, G.K., Speed, T.P., and White, K.P. (2006). Expression profiling in primates reveals a rapid evolution of human transcription factors. Nature *440*, 242–245.

Glinka, S., Ometto, L., Mousset, S., Stephan, W., and De Lorenzo, D. (2003). Demography and natural selection have shaped genetic variation in *Drosophila melanogaster*: a multi-locus approach. Genetics *165*, 1269–1278.

Haddrill, P.R., Thornton, K.R., Charlesworth, B., and Andolfatto, P. (2005). Multilocus patterns of nucleotide variability and the demographic and selection history of *Drosophila melanogaster* populations. Genome Res. *15*, 790–799.

Hancock, A.M., Witonsky, D.B., Alkorta-Aranburu, G., Beall, C.M., Gebremedhin, A., Sukernik, R., Utermann, G., Pritchard, J.K., Coop, G., and Di Rienzo, A. (2011). Adaptations to climate-mediated selective pressures in humans. PLoS Genet. *7*, e1001375.

Hansen, T.F. (1997). Stabilizing selection and the comparative analysis of adaptation. Evolution *51*, 1341–1351.

Held, T., Nourmohammad, A., and Lässig, M. (2014). Adaptive evolution of molecular phenotypes. J. Stat. Mech. *9*, P09029.

Hoekstra, H.E., and Coyne, J.A. (2007). The locus of evolution: evo devo and the genetics of adaptation. Evolution *61*, 995–1016.

Ikemura, T. (1985). Codon usage and tRNA content in unicellular and multicellular organisms. Mol. Biol. Evol. *2*, 13–34.

Khaitovich, P., Weiss, G., Lachmann, M., Hellmann, I., Enard, W., Muetzel, B., Wirkner, U., Ansorge, W., and Pääbo, S. (2004). A neutral model of transcriptome evolution. PLoS Biol. *2*, E132.

Khaitovich, P., Hellmann, I., Enard, W., Nowick, K., Leinweber, M., Franz, H., Weiss, G., Lachmann, M., and Pääbo, S. (2005). Parallel patterns of evolution in the genomes and transcriptomes of humans and chimpanzees. Science *309*, 1850–1854.

King, M.C., and Wilson, A.C. (1975). Evolution at two levels in humans and chimpanzees. Science *188*, 107–116.

Lachaise, D., Cariou, M., David, J., Lemeunier, F., Tsacas, L., and Ashburner, M. (1988). Historical biogeography of the *Drosophila melanogaster* species subgroup. In Evolutionary Biology, *Volume 22*, M. Hecht, B. Wallace, and G. Prance, eds. (Springer), pp. 159–225.

Leinonen, T., McCairns, R.J., O'Hara, R.B., and Merilä, J. (2013). Q(ST)-F(ST) comparisons: evolutionary and ecological insights from genomic heterogeneity. Nat. Rev. Genet. *14*, 179–190.

Lemos, B., Meiklejohn, C.D., Cáceres, M., and Hartl, D.L. (2005). Rates of divergence in gene expression profiles of primates, mice, and flies: stabilizing selection and variability among functional categories. Evolution *59*, 126–137.

Lynch, M., and Hill, W.G. (1986). Phenotypic evolution by neutral mutation. Evolution *40*, 915–935.

McDonald, J.H., and Kreitman, M. (1991). Adaptive protein evolution at the Adh locus in *Drosophila*. Nature *351*, 652–654.

Mustonen, V., and Lässig, M. (2007). Adaptations to fluctuating selection in *Drosophila*. Proc. Natl. Acad. Sci. USA *104*, 2277–2282.

Mustonen, V., and Lässig, M. (2010). Fitness flux and ubiquity of adaptive evolution. Proc. Natl. Acad. Sci. USA *107*, 4248–4253.

Nourmohammad, A., Held, T., and Lässig, M. (2013a). Universality and predictability in molecular quantitative genetics. Curr. Opin. Genet. Dev. *23*, 684–693.

Nourmohammad, A., Schiffels, S., and Lässig, M. (2013b). Evolution of molecular phenotypes under stabilizing selection. J. Stat. Mech. *1*, P01012.

Orr, H.A. (1998). Testing natural selection vs. genetic drift in phenotypic evolution using quantitative trait locus data. Genetics *149*, 2099–2104.

Pai, A.A., Pritchard, J.K., and Gilad, Y. (2015). The genetic and mechanistic basis for variation in gene regulation. PLoS Genet. *11*, e1004857.

Quackenbush, J. (2002). Microarray data normalization and transformation. Nat. Genet. *32* (*Suppl*), 496–501.

Riedel, N., Khatri, B.S., Lässig, M., and Berg, J. (2015). Multiple-line inference of selection on quantitative traits. Genetics *201*, 305–322.

Rifkin, S.A., Kim, J., and White, K.P. (2003). Evolution of gene expression in the *Drosophila melanogaster* subgroup. Nat. Genet. *33*, 138–144.

Rifkin, S.A., Houle, D., Kim, J., and White, K.P. (2005). A mutation accumulation assay reveals a broad capacity for rapid evolution of gene expression. Nature *438*, 220–223.

Romero, I.G., Ruvinsky, I., and Gilad, Y. (2012). Comparative studies of gene expression and the evolution of gene regulation. Nat. Rev. Genet. *13*, 505–516.

Sella, G., Petrov, D.A., Przeworski, M., and Andolfatto, P. (2009). Pervasive natural selection in the *Drosophila* genome? PLoS Genet. *5*, e1000495.

Shields, D.C., Sharp, P.M., Higgins, D.G., and Wright, F. (1988). "Silent" sites in *Drosophila* genes are not neutral: evidence of selection among synonymous codons. Mol. Biol. Evol. *5*, 704–716.

Stephan, W., and Li, H. (2007). The recent demographic and adaptive history of *Drosophila melanogaster*. Heredity (Edinb) *98*, 65–68.

Sunyaev, S.R., and Roth, F.P. (2013). Systems biology and the analysis of genetic variation. Curr. Opin. Genet. Dev. *23*, 599–601.

Thornton, K.R., Jensen, J.D., Becquet, C., and Andolfatto, P. (2007). Progress and prospects in mapping recent selection in the genome. Heredity (Edinb) *98*, 340–348.

Whitehead, A., and Crawford, D.L. (2006). Neutral and adaptive variation in gene expression. Proc. Natl. Acad. Sci. USA *103*, 5425–5430.

Wittkopp, P.J., Haerum, B.K., and Clark, A.G. (2008). Regulatory changes underlying expression differences within and between *Drosophila* species. Nat. Genet. *40*, 346–350.

Wright, F. (1990). The effective number of codons used in a gene. Gene *87*, 23–29.

Zhang, Y., Sturgill, D., Parisi, M., Kumar, S., and Oliver, B. (2007). Constraint and turnover in sex-biased gene expression in the genus *Drosophila*. Nature *450*, 233–237.